

A simplified human birth model

Roseanna Gossmann^{1*}, Alexa Baumer², Lisa Fauci¹, Megan C. Leftwich²

Tulane University¹, The George Washington University²

Motivation

- When compared with Caesarean delivery, vaginal delivery is linked to
 - shorter post-birth hospital stays
 - lower likelihood of intensive care stays
 - lower mortality rates [1]



Greater understanding of the causes of force on the infant during childbirth could decrease the occurrence of unnecessary Caesarean deliveries. Fluid mechanics greatly informs the total mechanics of birth. [4] We aim to discover how the involved fluids affect forces on the infant during birth.

Experimental Parameters

- Rigid acrylic cylinder (fetus) pulled through center of passive elastic tube (birth canal)
- System immersed in methyl cellulose in water (amniotic fluid)
- Force needed to pull the acrylic cylinder at a prescribed velocity measured as a function of time

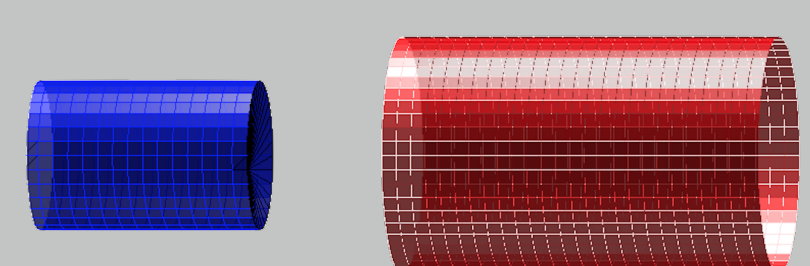


Physical experiment at Leftwich Laboratory²

Mathematical Background

- Much work has been done studying fluid flow through passive elastic tubes. [3]
- Tube dynamics have been modeled using nonlinear shell theory or elastic fiber network models, and fluid dynamics using lubrication theory and more complex fluid equations.
- Non-axisymmetric tube collapse occurs when the transmural pressure reaches a critically low value.

Numerical Simulation



Rigid inner cylinder (blue) will be translated through elastic tube with fixed ends (red), in boundless Stokes flow, pictured at simulation start time for one set of tube/rod dimensions.

Numerical Methods

Elastic tube

- Tube modeled by network of Hookean springs, with velocity $\mathbf{U} = \mathbf{0}$ at ends.
- Force at \mathbf{x}_I due to spring from \mathbf{x}_m :

$$\mathbf{g}(\mathbf{x}_I) = \tau \left(\frac{\|\mathbf{x}_m - \mathbf{x}_I\|}{\Delta_{lm}} - 1 \right) \frac{(\mathbf{x}_m - \mathbf{x}_I)}{\|\mathbf{x}_m - \mathbf{x}_I\|}$$
- τ chosen to match elastic properties to physical experiment. [5]

Rigid inner cylinder

- A time-dependent velocity $\mathbf{U}(t)$ is specified in the z -direction.

Fluid governed by the Stokes equations:

$$\mathbf{0} = -\nabla p + \mu \Delta \mathbf{u} + \sum_{k=1}^N \mathbf{f}_k, \quad \nabla \cdot \mathbf{u} = 0,$$

Algorithm

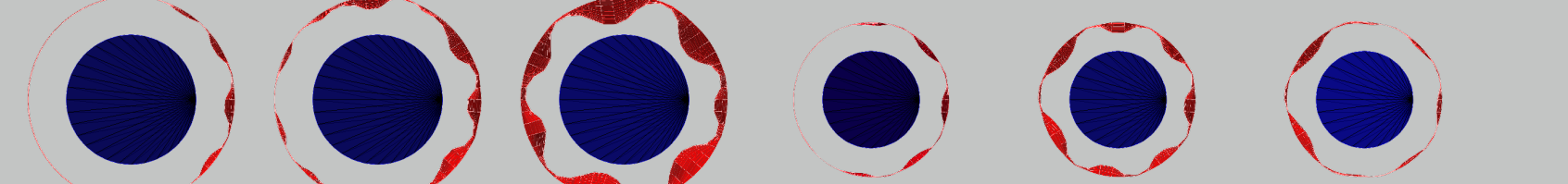
- find velocity on the tube ends and rod induced by spring forces,
- solve for additional forces necessary to achieve prescribed velocities,
- evaluate velocity and pressure throughout system,
- update position of all tube and rod using Forward Euler ($\mathbf{x} = \mathbf{x} + \mathbf{U}\Delta t$),
- repeat.

Tube Number and Its Effect on Elastic Buckling

We define the *tube number* as $\eta = \frac{\mu U R_T R_C L_C}{(R_T/L_T)\mathcal{E}I}$, where R_T, R_C are radii of tube and rod, L_T, L_C are lengths of tube and rod, U is rod velocity, $\mathcal{E}I$ is tube bending stiffness.

- When η is constant, tube buckling is identical for any values for $\mu, U, \mathcal{E}I$, as long as tube and rod dimensions are held constant. Changing the tube and rod geometry changes the elastic behavior.

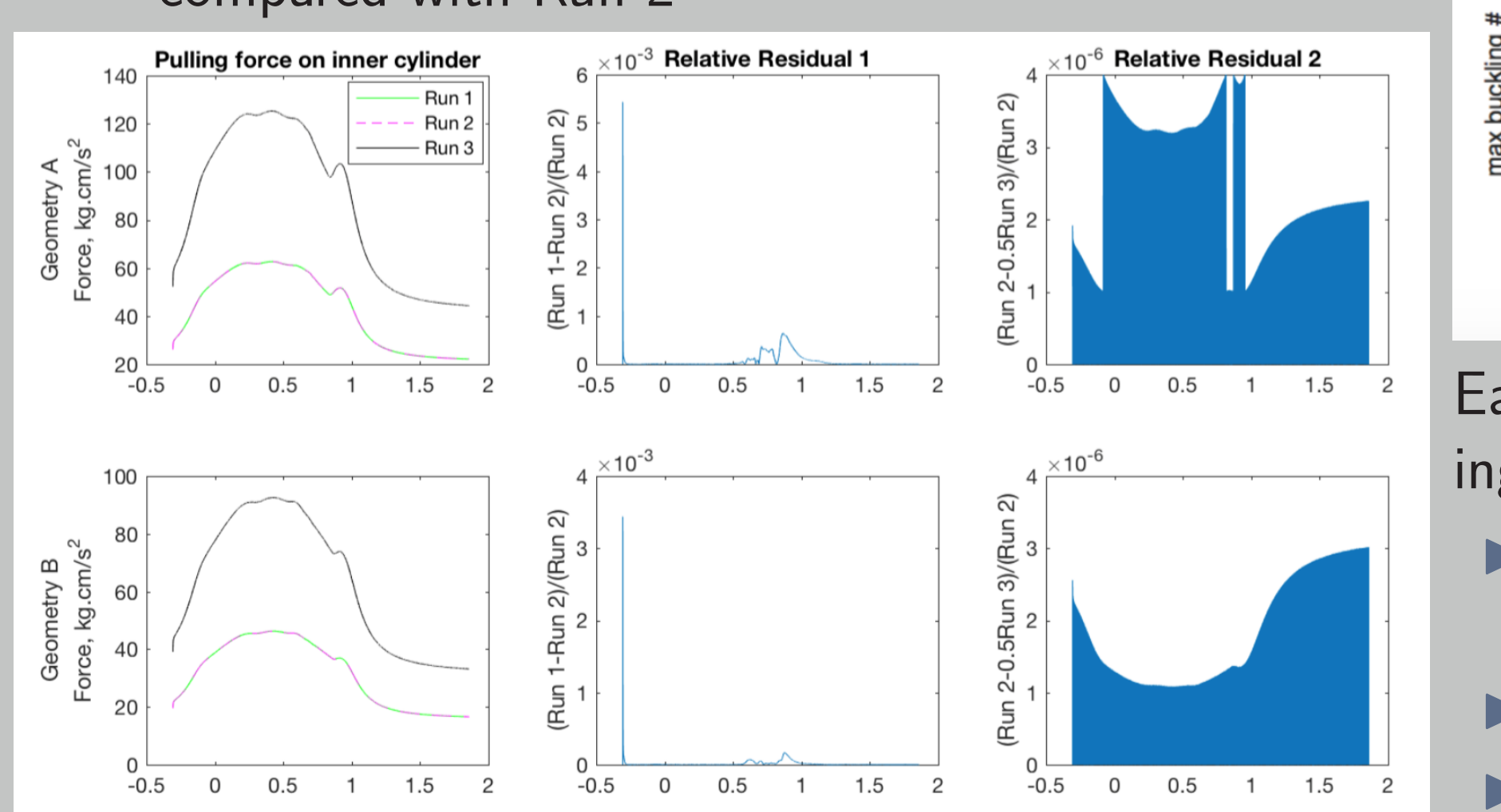
Geometry A, tube buckling over time:



Geometry B, tube buckling over time:

In general, nonlinear elastic behavior results in loss of proportional relationship between force and velocity.

- Dimensional analysis predicts that for constant η , $\mathbf{f} = \mathbf{C}\mu\mathbf{U}$ for constant \mathbf{C} .
- In simulations (see figure below) $\mathbf{f} = \mathbf{C}\mu\mathbf{U}$ holds true.
 - Run 2 has doubled U and halved μ compared with Run 1
 - Run 3 has doubled U with μ held constant compared with Run 2

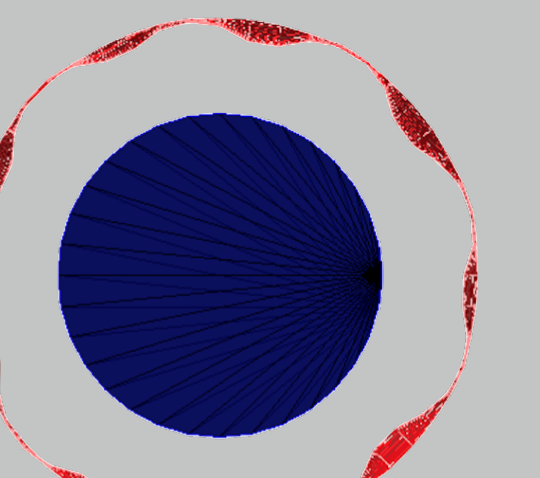


where \mathbf{f}_k is the total force on the point \mathbf{x}_k .

The linear relationship between fluid velocity and pressure and regularized forces localized at N points is given by

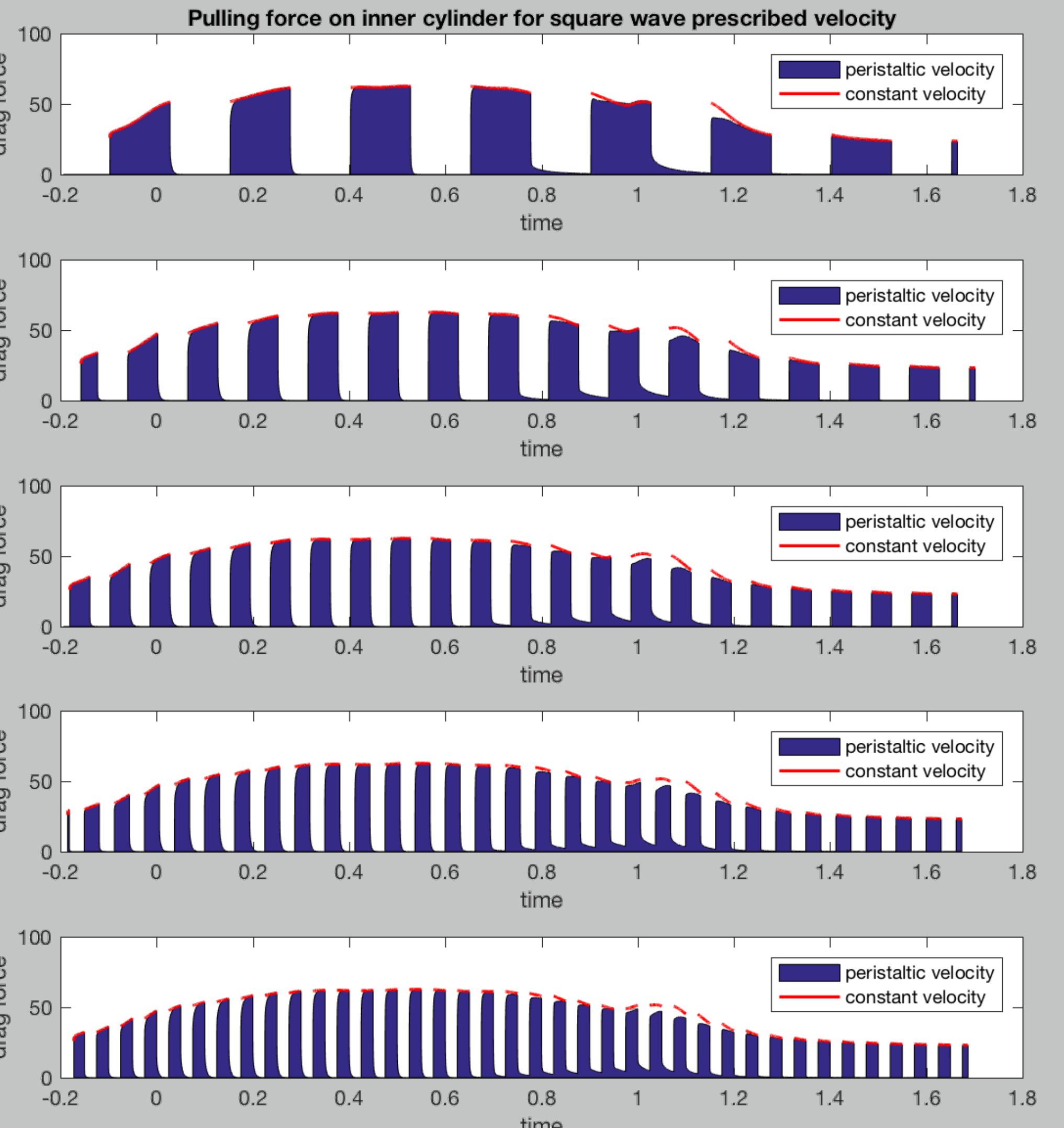
$$\begin{aligned} \mathbf{u}(\mathbf{x}) &= \frac{1}{\mu} \sum_{k=1}^N [(\mathbf{f}_k \cdot \nabla) \nabla B_\varepsilon(|\mathbf{x} - \mathbf{x}_k|) \\ &\quad - \mathbf{f}_k \mathbf{G}_\varepsilon(|\mathbf{x} - \mathbf{x}_k|)] + \mathbf{u}_b(\mathbf{x}), \\ \mathbf{p}(\mathbf{x}) &= \sum_{k=1}^N [\mathbf{f}_k \cdot \nabla \mathbf{G}_\varepsilon(|\mathbf{x} - \mathbf{x}_k|)], \end{aligned}$$

where $\Delta B_\varepsilon = \mathbf{G}_\varepsilon$, $\Delta \mathbf{G}_\varepsilon = \phi_\varepsilon = \frac{15\varepsilon^4}{8\pi(r^2+\varepsilon^2)^{(7/2)}}$, μ = viscosity, ε regularization parameter. [2]



Elastic tube buckles as inner cylinder moves through it and causes fluid pressure drop, viewed from trailing end for one set of parameters.

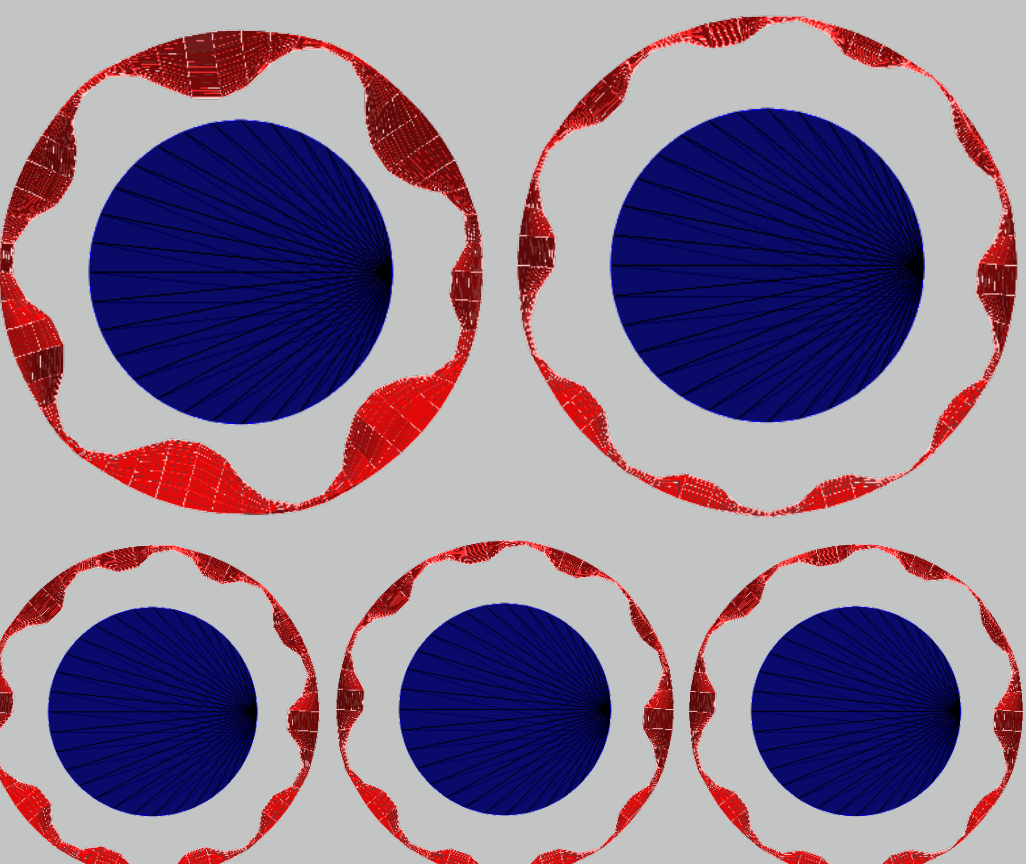
Modeling Peristalsis - Periodic Velocity



Square wave periodic velocity $\mathbf{U}(t)$ is compared with constant velocity input to mimic forces from peristaltic contraction.

- Force in 'peristaltic' case is equal to or less than the force at the same position in constant velocity case.

- Tube buckling for square wave velocity with max 0.4 (three cases in bottom row) is very similar to buckling for constant velocity 0.2 (top right), with depth variation due to start and stop of inner cylinder, and significantly different from buckling for constant velocity 0.4 (top left).



Future Work

- Develop elastic-body model for inner cylinder, allowing for prescription of forces rather than velocity.
- Activate elastic tube with peristaltic contractile forces.
- Explore effects of variable elastic properties across tube.
- Explore effect on force of axial alignment of cylinder inside tube.

References

- C. S. Buhimschi, I. A. Buhimschi, *Advantages of vaginal delivery*, Clinical obstetrics and gynecology 49 (1) (2006) 167-183.
- R. Cortez, L. Fauci, A. Medovikov, *The method of regularized Stokeslets in three dimensions: analysis, validation, and application to helical swimming*, Physics of Fluids (2005).
- J. B. Grotberg and O. E. Jensen, *Biofluid mechanics in flexible tubes*, Annual Review of Fluid Mechanics (2004) 36:121-147.
- A. M. Lehn, A. Baumer, M. C. Leftwich, *An experimental approach to a simplified model of human birth*, J Biomech. (2016).
- H. Nguyen and L. Fauci, *Hydrodynamics of diatom chains and semiflexible fibres*, J. R. Soc. Interface 11: 20140314 (2014).
- Fig.1: "HumanNewborn" by Ernest F - Own work. Licensed under CC BY-SA 3.0 via Commons - <https://commons.wikimedia.org/wiki/File:HumanNewborn.JPG>; "Postpartum baby2" by Tom Adriaensen - <http://www.flickr.com/photos/inferis/110652572/>. Licensed under CC BY-SA 2.0 via Commons - https://commons.wikimedia.org/wiki/File:Postpartum_baby2.jpg